# Shear wave elastography using high frame rate imaging in the follow-up of heart transplant recipients

Aniela Petrescu, MD[1)2)3)], Stéphanie Bézy, MSc[1)2)], Marta Cvijic, MD, PhD[1)2)], Pedro Santos, PhD[1)], Marta Orlowska, MSc[1)], Jürgen Duchenne, PhD[1)2)], João Pedrosa, PhD[1)], Jan M. Van Keer, MD[1)2)], Eric Verbeken, MD, PhD[4)], Stephan von Bardeleben, MD[3)], Walter Droogne, MD[1)2)], Jan Bogaert, MD, PhD[5)], Johan Van Cleemput, MD, PhD[1)2)], Jan D'hooge, PhD[1)*], Jens-Uwe Voigt, MD, PhD[1)2)*]

1) Department of Cardiovascular Sciences, University of Leuven, Leuven, Belgium
2) Department of Cardiovascular Diseases, University Hospitals Leuven, Leuven, Belgium
3) Department of Cardiology, Mainz University Hospital, University of Mainz, Mainz, Germany
4) Translational Cell and Tissue Research, Department of Imaging and Pathology, University of Leuven, Leuven, Belgium
5) Radiology Department, University Hospitals Leuven, Leuven, Belgium

*Jan D'hooge and Jens-Uwe Voigt share senior authorship.

**Total word count: 4974**
**Brief title: Shear wave imaging in heart transplant recipients**

**Corresponding author contact information**
Prof. Dr. Jens-Uwe Voigt
University Leuven and University Hospitals Leuven
Herestraat 49, 3000 Leuven, Belgium
Tel.: +32 / 16 / 349016
Email: jens-uwe.voigt@uzleuven.be

**ACKNOWLEDGMENTS:**
This work was supported by the European Research Council (FP7/2007-2013, ERC/281748) and the Research Foundation - Flanders (FWO/G002617N, FWO/G092318N). Aniela Petrescu was supported by a German Society of Cardiology Research Grant and Marta Cvijic by a European Association of Cardiovascular Imaging Research Grant. The authors are grateful to Vangjush Komini, Bidisha Chakraborty, Ganna Degtiarova and Monica Dobrovie for their support.

**Key Words:** high frame rate echocardiography; shear wave; myocardial stiffness; heart transplant;

## STRUCTURED ABSTRACT

**Background:** After orthotopic heart transplantation (HTx), allografts undergo diffuse myocardial injury (DMI) that contributes to functional impairment, especially to increased passive myocardial stiffness, which is an important pathophysiological determinant of left ventricular (LV) diastolic dysfunction. Echocardiographic shear wave (SW) elastography is an emerging approach for measuring myocardial stiffness in vivo. Natural SWs occur after mechanical excitation of the myocardium, e.g. after mitral valve closure (MVC) and their propagation velocity is directly related to myocardial stiffness, thus providing an opportunity to assess myocardial stiffness at end-diastole.

**Objectives:** To investigate if propagation velocities of naturally occurring SWs at MVC increase with the degree of DMI and with invasively determined LV filling pressures as a reflection of an increase in myocardial stiffness in HTx recipients.

**Methods:** 52 HTx recipients that underwent right heart catheterization (all) and cardiac magnetic resonance (CMR, n=23) during their annual check-up were prospectively enrolled. Echocardiographic SW elastography was performed in parasternal long axis views of the LV using an experimental scanner at 1135 ± 270 frames per second. The degree of DMI was quantified with T1 mapping.

**Results:** SW velocity at MVC correlated best with native myocardial T1 values ($r=0.80$, $p<0.0001$) and was the best non-invasive parameter to correlate with pulmonary capillary wedge pressures (PCWP; $r=0.54$, $p<0.001$). Standard echocardiographic parameters of LV diastolic function correlated poorly with both native T1 values and PCWP.

**Conclusions:** End-diastolic shear wave propagation velocities, as measure of myocardial stiffness, showed a good correlation with CMR defined diffuse myocardial injury and with invasively determined left ventricular filling pressures in HTx patients. These findings thus suggest that shear wave elastography has the potential to become a valuable non-invasive method for the assessment of diastolic myocardial properties in heart transplant recipients.

## CONDENSED ABSTRACT

By using high-frame rate imaging we investigated if shear waves velocities can detect the change in passive myocardial stiffness that occurs in heart transplant recipients due to diffuse myocardial injury. We could show that end-diastolic shear wave velocities correlated best with native CMR T1 times of the myocardium as marker of diffuse myocardial injury, and were the best non-invasive parameter to correlate with pulmonary wedge pressures measurements, as a reflection of an increase in left ventricular filling pressures. Therefore, shear wave imaging could become a non-invasive tool for the assessment of passive diastolic myocardial properties in heart transplant recipients.

## ABBREVIATIONS LIST

| | |
|---|---|
| CMR | cardiac magnetic resonance |
| E/E' | mitral inflow to mitral relaxation velocity ratio |
| ED | end-diastole |
| ECV | extracellular volume |
| HFR | high frame rate |
| HTx | heart transplant |
| LGE | late gadolinium enhancement |
| LV | left ventricle |
| MVC | mitral valve closure |
| SW | shear wave |
| PCWP | pulmonary capillary wedge pressure |

# INTRODUCTION

After heart transplantation (HTx), some recipients may develop allograft dysfunction, which is associated with poor outcome (1) and which is supposed to be the result of myocardial damage caused by prolonged ischemic time during transplantation, donor-specific antibodies, rejection episodes, hypertension, vasculopathy or immunosuppressive therapy (2). A common pathophysiologic pathway involves histologic alterations such as myocyte hypertrophy and diffuse myocardial fibrosis that contribute to increased myocardial stiffness, an important determinant of ventricular diastolic dysfunction (3,4). Given the importance of early detection of graft dysfunction, tissue characterization and assessment of diastolic function are major aims of the routine evaluation in HTx recipients.

Right heart catheterization is a standard method for the follow-up of HTx patients, allowing the invasive measurements of pulmonary pressures and pulmonary capillary wedge-pressures to estimate diastolic allograft function(5). Nevertheless, being an invasive and not risk-free procedure, catheterizations have to be limited and are frequently triggered by non-invasive signs of graft dysfunction.

Cardiac magnetic resonance (CMR) with late gadolinium enhancement (LGE) imaging is the reference method for detecting focal myocardial fibrosis in the clinical practice, but it cannot detect subtle and diffuse myocardial abnormalities. Diffuse myocardial injury can be characterized through mapping of T1 relaxation times (3,6,7). The expansion of the extracellular matrix (extracellular volume, ECV) can be calculated from native and post-contrast T1 time while native T1 time reflects myocardial disease involving both myocytes and interstitial space (7,8). However, despite its capability for tissue characterization, CMR has the disadvantage of high costs, low availability and limited feasibility in patients with arrhythmias or implants.

Echocardiography is routinely performed in patients after HTx. The interpretation of echocardiographic parameters of diastolic function, however, is particularly difficult in these patients and does not allow for differentiation between impaired active relaxation, passive stiffness and other factors (e.g. volume loading, extrinsic factors) that may contribute to diastolic dysfunction (9).

Cardiac shear wave imaging using high frame rate (HFR) echocardiography is an emerging noninvasive method for the assessment of myocardial properties. Shear waves (SW) are mechanical waves that can be artificially induced by the radiation force of a focused ultrasound impulse (10,11), but can also originate from physiologic events, such as aortic and mitral valve closure (MVC) (12,13). The speed of SW propagation depends directly on myocardial stiffness and typically ranges between 1 and 10 m/s. Myocardial SWs are short-lived events and attenuate quickly, therefore high frame rate imaging (more than 1000 frames per second) is required for their proper assessment (13). The technique has been validated in phantoms (14) and increased SW propagation velocities have been demonstrated with ageing, as well as in pathology such as cardiac amyloidosis, hypertrophic cardiomyopathy and arterial hypertension. Moreover, SW velocities at MVC (at end-diastole), have been shown to correlate with the filling pressures of the left ventricle (LV) (11,14,15).

Given the above-mentioned clinical need for non-invasive parameters that reflect diffuse myocardial injury and which can be used for risk stratification in HTx patients, we investigated the potential of estimating passive myocardial stiffness in HTx patients by natural SW imaging. Findings were compared to CMR T1 mapping parameters, invasive measurements by right heart catheterization and standard echocardiographic parameters of diastolic function.

## METHODS

### *Study population*

We prospectively enrolled 52 HTx recipients (9.9±6.4 years after HTx), which had been referred for the routine yearly follow-up right heart catheterization to the Department of Cardiovascular Diseases of the University Hospital Gasthuisberg, Leuven between May 2018 and February 2019. Exclusion criteria comprised ventricular pacing, left bundle branch block, atrioventricular block more than first degree, histological or clinical evidence of allograft rejection, significant left coronary artery stenosis, more than moderate valvular disease, and poor echogenicity.

All participants underwent standard echocardiography, echocardiographic SW imaging and right heart catheterization within 24 hours. In 23 patients, recent CMR data were available without evidence for acute cardiac events between the time point of CMR and the study examinations.

The study was approved by the Ethical Committee of the University Hospital Leuven and written informed consent was obtained from all participants.

### *Standard Echocardiography*

Standard echocardiographic examinations were performed with a Vivid E9 system (GE Vingmed Ultrasound, Horten, Norway). Digitally stored data were analyzed offline using EchoPAC PC software (Version 202, GE Vingmed Ultrasound, Horten, Norway). The routine parameters comprised left heart volumes and ejection fraction, assessed with the biplane Simpson method (16), mitral inflow E/A ratio, deceleration time, isovolumetric relaxation time, tissue Doppler E/E' ratio (E/E'), and an estimate of systolic pulmonary artery pressure

as the peak gradient of tricuspid regurgitation (9). Furthermore, LV global longitudinal strain was measured using Speckle Tracking.

***Shear Wave imaging***

SW imaging was performed with a custom made, fully programmable experimental scanner (HD-PULSE), equipped with a clinical phased array transducer (Samsung Medison P2-5AC). Our protocol has been previously validated in phantoms and has been described in detail in the online Supplement (14).

In summary, a parasternal long axis view of the heart was acquired with diverging transmit waves leading to fast image sequences at 1135 ± 270 frames per second. Tissue acceleration was calculated from the tissue Doppler velocity estimates from the HFR data. Anatomical acceleration M-mode maps were extracted along the midline of the LV septum. The SWs of interest, appearing on the M-mode as tilted color bands, were identified after MVC as time reference for end-diastole (ED) and their slopes were measured semi-automatically (**Central Illustration**). Data were analysed by two independent observers, who were blinded to any clinical information. All SW propagation velocity measurements were repeated three times and results were averaged.

***Cardiac magnetic resonance***

CMR was performed on a clinical 1.5-Tesla scanner (Ingenia; Philips Healthcare, Erlangen, Germany) by using commercially available CMR imaging software, electrocardiographic triggering, and a cardiac-dedicated phase array coil. The protocol started with Steady-state free-precession breath-hold cine images that were acquired in the vertical and horizontal long-axis, short axis and left ventricular outflow tract view. In order to assess regional myocardial fibrosis, 3-dimensional phase-sensitive inversion recovery gradient

(PSIR) gradient-echo sequences for late-enhancement were performed in all available slices after gadobutrol administration, as previously described in detail(17). To evaluate the degree of diffuse myocardial injury (i.e myocyte hypertrophy and diffuse myocardial fibrosis), native T1 mapping was performed using a modified Look-Locker inversion recovery sequence before gadobutrol application on three short-axis slices (basal, mid and apical). For each short-axis image, a region of interest was drawn in the anteroseptal wall to calculate myocardial T1 time as average of all involved slices **(Central Illustration)**. Postcontrast T1 was obtained 15 minutes after gadobutrol application in all available slices, and ECV was derived as previously described (18).

Since prolonged T2 relaxation has been related to transplant edema and possibly rejection, T2 mapping sequences were assessed in mid-ventricular short-axis slices in order to exclude patients with acute transplant rejection (19). All images were interpreted by an experienced reader blinded to any other data of the patients.

***Right heart catheterization***

Right heart catheterization was performed using a Swan-Ganz pulmonary artery thermodilution catheter (Edwards Lifesciences Corp, One Edwards Way, Irvine, CA). Pressure curves were recorded and a comprehensive hemodynamic assessment including pulmonary capillary wedge pressure (PCWP), systolic pulmonary artery pressure, mean right atrial pressure, cardiac output and pulmonary vascular resistance was performed. To ensure consistency, the parameters used for data analysis were those automatically measured and averaged by the hemodynamic system (Sensis, Siemens Healthcare GmbH, Erlangen, Germany) over 10 seconds during shallow breathing.

***Statistical analysis***

Continuous parameters are presented as means ± standard deviation when normally distributed and otherwise as median and quartile. Categorical variables are presented as frequencies and percentages. Normal distribution was tested using the Shapiro-Wilk test. The association of variables was expressed using Pearson's correlation coefficient. In order to minimize the effect of an outlier, the association of T1 values with other parameters was expressed using Spearman's correlation. Inter- and intra-observer variability was evaluated in 15 patients using intra-class correlation coefficient (two-way mixed model, absolute agreement between single measures) and Bland-Altman analysis. Receiver-operating characteristics curves were constructed to assess optimal cut-off value for the SW velocities to predict native T1 relaxation time>1040 ms and PCWP>15 mmHg. All statistical analyses were performed using SPSS Statistics Software (Version 25.0, IBM, Chicago, IL). A two-sided P value of 0.05 was considered statistically significant for all tests.

## RESULTS

*Study population*

A total of 52 HTx recipients without clinical evidence of acute rejection were prospectively enrolled in the study. Two patients had bad echogenicity, one a histologic proof of acute rejection, two patients had significant left coronary artery stenosis, and one had biopsy showing recurrence of AL amyloidosis. Finally, 46 patients (mean age 54.1±17.8 years, 78% male) could be included in the analysis. Patient characteristics including clinical data, echocardiography, CMR and invasive measurements are reported in **Table 1**.

*Feasibility and Reproducibility of myocardial SW velocity measurements*

Myocardial SWs after MVC (at ED) were detected in 42 patients (91%) with a mean SW velocity of 5.00 ± 2.04 m/s. SW velocity measurements showed a good intra-observer and inter-observer reproducibility by using both intra-class correlation coefficient (intra-class correlation coefficients 0.93; 95% CI, 0.81-0.98 and 0.93; 95% CI, 0.81-0.98, respectively) and Bland-Altman plots (**Figure 1).**

*SW velocities and parameters of diastolic function*

We found a significant correlation between SW propagation velocities and invasive PCWP measurements (r=0.54, p<0.001, **Figure 2A**). SW velocities above a cut-off of 5.14 m/s (sensitivity 71%, specificity 84%, area under the curve=0.72) showed the highest accuracy to identify patients with PCWP higher than 15 mmHg (**Figure 3A**). Standard echocardiographic measures of LV diastolic function correlated poorly with SW velocities (E/E': r =0.34, p=0.03; deceleration time: r=-0.46, p=0.003; left atrial volume: r=0.35, p=0.03). No correlation was found between SW velocities and mitral inflow E/A ratio

(r=0.18, p=0.28) or isovolumetric relaxation time (r=0.03, p=0.87). Similarly, the linear relation between PCWP and standard echocardiographic estimates of diastolic function was weak to moderate **(Table 2).**

*CMR measurements*

Twenty-three patients underwent CMR. Time between CMR and echo was typically 4 months (in average 4.3 ± 4.9 months). Results are displayed in **Table 1**. LGE of non-ischemic pattern was observed in five patients (22%): two patients had subepicardial basal lateral and basal septal LGE, respectively, one patient had pericardial LGE, one patient had patchy LGE most pronounced in the basal segments, and one patient had focal apical LGE. The native T1 time in the anteroseptal wall could be assessed in 22 (96%) patients and ECV was calculated in 20 (87%) patients after gadolinium injection. T2 mapping was performed in 20 patients (87%) and showed normal myocardial T2 values ensuring that no patient had acute graft rejection.

*Correlates of diffuse myocardial injury by CMR*

The increase of both SW velocities and PCWP was accompanied by an increase in T1 values (**Figure 2B**). Significant correlation was observed between native myocardial T1 times and SW velocities (r=0.75, p=0.0001) **(Figure 4A).** SW velocities above 4.84 m/s could identify T1 times > 1040ms with a sensitivity and specificity of 82% and 82 %, resp. (area under the curve=0.81) **(Figure 3B)**. The correlation between native T1 times and PCWP was r=0.63 (p=0.001, **Figure 4B**). Overall, moderate to poor correlations were observed between native T1 times and standard echocardiographic parameters of diastolic function **(Table 3)**, the correlation with E/E' – as well defined standard echocardiographic parameter for predicting filling pressures - being not significant (r=0.35, p=0.1, **Figure 4C**).

## DISCUSSION

After HTx, allografts may undergo diffuse myocardial injury such as myocyte hypertrophy and diffuse fibrosis that contribute to functional changes of the transplanted heart and are associated with poor outcome (1). They represent the morphological substrate of adverse ventricular remodeling and are potentially reversible under treatment (20). In this context, a widely available, non-invasive method to early detect diffuse myocardial changes in HTx patients may have an important value for risk stratification and therapy. In the current study, SW propagation velocities in the LV septum were non-invasively measured by HFR echocardiography and compared to invasive and non-invasive measures of diastolic function, as well as CMR-derived parameters. SW propagation velocities showed a good correlation with the degree of diffuse myocardial injury assessed by CMR T1 mapping and were the non-invasive echocardiographic parameter that correlated best with PCWP.

### *Myocardial stiffness in HTx recipients*

To our knowledge, this is the first study assessing myocardial stiffness in HTx recipients using non-invasive echocardiographic imaging of natural SWs. In our cohort, SW velocities at ED ranged from 2.5 to 11.4 m/s. The lower values compare to findings that we and others reported in healthy volunteers (13, 19), and the higher values have the same order of magnitude as the ones reported in patients with hypertension, cardiac amyloidosis and hypertrophic cardiomyopathy (11,14,15). Our findings therefore suggest also for HTx patients an association between altered myocardial tissue and increased myocardial stiffness.

*SW velocities and parameters of diastolic function*

In our cohort, classical echocardiographic criteria of diastolic dysfunction reflected poorly invasive hemodynamics. This had already been reported before and proposed to be due to the distorsion of atrial anatomy affecting both the atrial contribution to LV filling and the pulmonary venous flow, as well as the increased heart rate at rest leading to E/A fusion(21,22).

SW propagation velocity correlated better with LV filling pressure as estimated by PCWP, but the correlation was still moderate. Similarly, PCWP showed only a moderate correlation with the underlying changes of the myocardium reflected by T1 mapping which are the actual target of interest for the structural evaluation of the transplanted heart. SW propagation velocities, on the other hand, showed a comparable or even better correlation to myocardial changes. In patients with available CMR, we observed that the increase of both SW velocities and PCWP was accompanied by an increase in T1 values, reflecting the link between the diastolic function and the histological changes of the myocardium. These findings could open a path to a better and non-invasive evaluation of diastolic properties of the LV in HTx recipients.

*SW velocities and CMR parameters*

Native myocardial T1 measurements have previously been shown to correlate with the quantity of diffuse myocardial fibrosis and myocyte hypertrophy observed in endomyocardial biopsy specimens of patients with and without HTx (23,24). In the current study, SW velocities in the LV septum of HTx recipients correlated well with native T1 values while T1 alterations due to myocardial edema and inflammation could be excluded based on normal T2 mapping results (25).

The T1 mapping values measured in this study were in the same range as other values previously reported in HTx patients or other conditions associated with diffuse myocardial fibrosis (3,24,26,27) and higher than values reported in healthy volunteers (28). Therefore, considering previous literature and the reference values obtained at 1.5 T with the same methodology in healthy volunteers (997±17 ms for native T1 and 25±3% for ECV) reported by our group (29), 50% of our patients with available MRI had abnormally elevated T1 values of more than 1040 ms indicating the presence of diffuse myocardial injury. Therefore, since the CMR data covered a wide range of values, even by using a small cohort size, the relation between velocities of naturally occurring shear waves and diffuse myocardial injury and hence, myocardial stiffness, could be demonstrated in our HTx population.

*Study limitations*

There are several limitations to this study. Firstly, our method of SW elastography using natural occurring SWs is based on measurements in the interventricular septum and cannot be extrapolated to the entire ventricle. Nevertheless, myocardial changes in HTx patients are supposed to be diffuse, so that we can expect homogeneous changes in LV wall stiffness.

Secondly, SWs caused by MVC occur during isovolumetric contraction time where intracardiac pressures may show relevant changes. Our values therefore do not strictly represent ED myocardial properties.

PCWP is reported as widely accepted surrogate parameter of LV end-diastolic pressures (30) as left heart catheterization is not performed without clinical indication. Since right heart catheterization is the gold standard for diagnosis of the restrictive physiology post-HTx, all subjects included in this study underwent right heart catheterization as part of the routine yearly follow-up(31). In order to avoid relevant misinterpretation of LV filling

pressure, patients with significant mitral valvular disease or with atrial fibrillation were excluded.

CMR and other study investigations were not always performed at the same visit. However, all patients were clinically stable between the measurements without hospitalizations for cardiac and non-cardiac cause.

Finally, although our findings showed a significant relation between velocities of naturally occurring shear waves and diffuse myocardial injury, the sample size was relatively small.

Despite these clinical and technical limitations, it is clear that an important step has been made toward the non-invasive analysis of the diastolic myocardial properties in HTx patients. However, given the novelty of the method which requires prospective data acquisition, and the rather good long-term survival of HTx patients in general, outcome data are not yet available.

## CONCLUSIONS

The propagation velocity of end-diastolic natural shear waves showed a good correlation with CMR markers of diffuse fibrosis, and with invasively-determined left ventricular filling pressures, both reflecting the impact of chronic histologic changes on myocardial stiffness of heart transplant recipients. Our findings suggest that cardiac shear wave elastography has the potential to become a valuable non-invasive method for the assessment of diastolic myocardial properties providing a fast and cheap alternative to magnetic resonance imaging and invasive procedures.

## PERSPECTIVES

### COMPETENCY IN MEDICAL KNOWLEDGE

In our study, we observed that natural SW propagation velocities as measured by high frame rate echocardiography correlated best with CMR T1 values, showing the link between an altered composition of the myocardial tissue and its mechanical properties at ED. This correlation was stronger than the one between LV filling pressures and T1 and completely outperformed classical echocardiographic parameters of diastolic dysfunction. The emerging technology of SW imaging may therefore become a new, feasible, accessible and non-invasive tool for the follow-up of HTx patients.

### TRANSLATIONAL OUTLOOK

A single non-invasive parameter to assess ventricular stiffness as supposed mechanism of diastolic function in HTx recipients with evidence of diffuse myocardial injury has not been previously reported. Still today, estimation of diastolic function in this group of patients is based on invasive measurements. Shear wave imaging is an extremely promising approach, and additional studies are needed to clarify if this parameter could improve the diagnosis and prognosis of this population.

## REFERENCES


1. López-Sainz Á., Barge-Caballero E., Barge-Caballero G., et al. Late graft failure in heart transplant recipients: incidence, risk factors and clinical outcomes. Eur J Heart Fail 2018;20(2):385–94.
2. Pickering JG., Boughner DR., Robarts JP., Boughner DR. Fibrosis in the Transplanted Heart and Its Relation to Donor Ischemic Time Assessment With Polarized Light Microscopy and Digital Image Analysis. Circulation 1990; 81(3):949-58.
3. Ellims AH., Shaw J a., Stub D., et al. Diffuse myocardial fibrosis evaluated by post-contrast t1 mapping correlates with left ventricular stiffness. J Am Coll Cardiol 2014:1112–8. Doi: 10.1016/j.jacc.2013.10.084.
4. Rowan RA., Billingham ME. Pathologic changes in the long-term transplanted heart: a morphometric study of myocardial hypertrophy, vascularity, and fibrosis. Hum Pathol 1990;21(7):767–72.
5. Lim HS., Hsich E., Shah KB. International Society of Heart and Lung Transplantation position statement on the role of right heart catheterization in the management of heart transplant recipients. J Hear Lung Transplant 2019;38(3):235–8. Doi: 10.1016/J.HEALUN.2018.12.009.
6. Bull S., White SK., Piechnik SK., et al. Original article: Human non-contrast T1 values and correlation with histology in diffuse fibrosis. Heart 2013;99(13):932. Doi: 10.1136/HEARTJNL-2012-303052.
7. Riesenkampff E., Chen CK., Kantor PF., et al. Diffuse Myocardial Fibrosis in Children After Heart Transplantations. Transplantation 2015;99(12):2656–62. Doi: 10.1097/TP.0000000000000769.
8. Moon JC., Treibel TA., Schelbert EB. T1mapping for diffuse myocardial fibrosis: A key biomarker in cardiac disease? J Am Coll Cardiol 2013;62(14):1288–9. Doi:

10.1016/j.jacc.2013.05.077.

9. Nagueh SF., Smiseth OA., Appleton CP., et al. Recommendations for the Evaluation of Left Ventricular Diastolic Function by Echocardiography: An Update from the American Society of Echocardiography and the European Association of Cardiovascular Imaging. J Am Soc Echocardiogr 2016;29:277–314. Doi: 10.1016/j.echo.2016.01.011.
10. Pernot M., Lee WN., Bel A., et al. Shear Wave Imaging of Passive Diastolic Myocardial Stiffness: Stunned Versus Infarcted Myocardium. JACC Cardiovasc Imaging 2016; 9(9):1023-1030.
11. Villemain O., Correia M., Mousseaux E., et al. Myocardial Stiffness Evaluation Using Noninvasive Shear Wave Imaging in Healthy and Hypertrophic Cardiomyopathic Adults. JACC Cardiovasc Imaging 2018. Doi: 10.1016/j.jcmg.2018.02.002.
12. Santos P., Petrescu A., Pedrosa J., et al. Natural shear wave imaging in the human heart: normal values, feasibility and reproducibility. IEEE Trans Ultrason Ferroelectr Freq Control 2018:1–1. Doi: 10.1109/TUFFC.2018.2881493.
13. Cikes M., Tong L., Sutherland GR., D'Hooge J. Ultrafast cardiac ultrasound imaging: Technical principles, applications, and clinical benefits. JACC Cardiovasc Imaging 2014;7(8):812–23. Doi: 10.1016/j.jcmg.2014.06.004.
14. Petrescu A., Santos P., Orlowska M., et al. Velocities of Naturally Occurring Myocardial Shear Waves Increase With Age and in Cardiac Amyloidosis. JACC Cardiovasc Imaging 2019. Doi: 10.1016/j.jcmg.2018.11.029.
15. Cvijic M., Bézy S., Petrescu A., et al. Interplay of cardiac remodelling and myocardial stiffness in hypertensive heart disease. Eur Heart J Cardiovasc Imaging 2020 ;21(6):664-672. Doi: 10.1093/ehjci/jez205.
16. Lang RM., Badano LP., Mor-Avi V., et al. Recommendations for Cardiac Chamber

Quantification by Echocardiography in Adults: An Update from the American Society of Echocardiography and the European Association of Cardiovascular Imaging. J Am Soc Echocardiogr 2015;28(1):1-39.e14. Doi: 10.1016/J.ECHO.2014.10.003.

17. Barreiro-Pérez M., Curione D., Symons R., Claus P., Voigt JU., Bogaert J. Left ventricular global myocardial strain assessment comparing the reproducibility of four commercially available CMR-feature tracking algorithms. Eur Radiol 2018;28(12):5137–47. Doi: 10.1007/s00330-018-5538-4.
18. Jellis CL., Kwon DH. Myocardial T1 mapping: modalities and clinical applications. Cardiovasc Diagn Ther 2014;4(2):126–12637. Doi: 10.3978/j.issn.2223-3652.2013.09.03.
19. Vermes E., Pantaléon C., Auvet A., et al. Cardiovascular magnetic resonance in heart transplant patients: Diagnostic value of quantitative tissue markers: T2 mapping and extracellular volume fraction, for acute rejection diagnosis. J Cardiovasc Magn Reson 2018;20(1). Doi: 10.1186/s12968-018-0480-9.
20. Armstrong AT., Binkley PF., Baker PB., David Myerowitz P., Leier C V. Quantitative Investigation of Cardiomyocyte Hypertrophy and Myocardial Fibrosis Over 6 Years After Cardiac Transplantation. J Am Coll Cardiol 1998; 32(3):704-10.
21. Broch K., Al-Ani A., Gude E., Gullestad L., Aakhus S. Scandinavian Cardiovascular Journal Echocardiographic evaluation of left ventricular filling pressure in heart transplant recipients Echocardiographic evaluation of left ventricular filling pressure in heart transplant recipients Echocardiographic evaluat. Scand Cardiovasc J 2014;48(6):349–56. Doi: 10.3109/14017431.2014.981579.
22. Okada DR., Molina MR., Kohari M., et al. Clinical echocardiographic indices of left ventricular diastolic function correlate poorly with pulmonary capillary wedge pressure at 1 year following heart transplantation Int J Cardiovasc Imaging 2015;31(4):783-94.

doi: 10.1007/s10554-015-0624-z. Epub 2015 Feb 21.

23. Bull S., White SK., Piechnik SK., et al. Human non-contrast T1 values and correlation with histology in diffuse fibrosis. Heart 2013;99(13):932–7. Doi: 10.1136/heartjnl-2012-303052.

24. Ide S., Riesenkampff E., Chiasson DA., et al. Histological validation of cardiovascular magnetic resonance T1 mapping markers of myocardial fibrosis in paediatric heart transplant recipients. J Cardiovasc Magn Reson 2017;19(1):1–11. Doi: 10.1186/s12968-017-0326-x.

25. Montant P., Sigovan M., Revel D., Douek P. MR imaging assessment of myocardial edema with T2 mapping. Diagn Interv Imaging 2015;96(9):885–90. Doi: 10.1016/j.diii.2014.07.008.

26. Kockova R., Kacer P., Pirk J., et al. Native T1 relaxation time and extracellular volume fraction as accurate markers of diffuse myocardial fibrosis in heart valve disease: Comparison with targeted left ventricular myocardial biopsy. Circ J 2016;80(5):1202–9. Doi: 10.1253/circj.CJ-15-1309.

27. aus dem Siepen F., Buss SJ., Messroghli D., et al. T1 mapping in dilated cardiomyopathy with cardiac magnetic resonance: quantification of diffuse myocardial fibrosis and comparison with endomyocardial biopsy. Eur Heart J Cardiovasc Imaging 2015;16(2):210–6. Doi: 10.1093/ehjci/jeu183.

28. Gottbrecht M., Kramer CM., Salerno M. Native T1 and Extracellular Volume Measurements by Cardiac MRI in Healthy Adults: A Meta-Analysis. Radiology 2019;290(2):317-326. doi: 10.1148/radiol.2018180226.

29. Degtiarova G., Gheysens O., Van Cleemput J., Wuyts W., Bogaert J. Natural evolution of cardiac sarcoidosis in an asymptomatic patient: A case report. Eur Hear J - Case Reports 2019;3(3). Doi: 10.1093/ehjcr/ytz099.

30. Reddy YN V., El-Sabbagh A., Nishimura RA. Comparing Pulmonary Arterial Wedge Pressure and Left Ventricular End Diastolic Pressure for Assessment of Left-Sided Filling Pressures. JAMA Cardiol 2018;3(6):453–4. Doi: 10.1001/JAMACARDIO.2018.0318.

31. Mehra MR., Crespo-Leiro MG., Dipchand A., et al. International Society for Heart and Lung Transplantation working formulation of a standardized nomenclature for cardiac allograft vasculopathy-2010. J Hear Lung Transplant 2010;29(7):717–27. Doi: 10.1016/j.healun.2010.05.017.

## FIGURE LEGENDS

**Central Illustration: T1 mapping of mid left ventricular segment of the anteroseptal wall and acceleration M-mode map of the anteroseptal wall in three heart transplant recipients (HTx1-3).** Note that shear wave velocities at mitral valve closure (MVC) increase with increasing native T1 value. The highlighted region of the ECG indicates the time interval covered by the M-mode map. HTx = heart transplant recipient; MVC = mitral valve closure.

**Figure 1: Bland-Altman plots for the intra-observer (A) and inter-observer (B) variability of the shear wave velocity measurements.** The bias is shown by the green dotted line, and the levels of agreement (1.95 x SD) by the dotted red lines.

**Figure 2: Shear wave propagation velocity and pulmonary capillary wedge pressure.** (A) Correlation between shear wave (SW) velocity propagation and pulmonary capillary wedge pressure (PCWP) in all patients. (B) Correlation between SW propagation velocity and PCWP in patients with CMR: SW velocities reflect the histological changes of the left ventricular myocardium as quantified by native T1. Note that the markers are coloured individually according to native T1 values. SW = shear wave; PCWP = pulmonary capillary wedge pressure.

**Figure 3**: **(A) Receiver-operating Curve (ROC) of SW propagation velocities for the detection of diffuse myocardial fibrosis as defined by T1>1040ms. (B) Same ROC analysis for the detection of increased filling pressures defined by PCWP>15 mmHg.**

**Figure 4: Diffuse myocardial injury assessed with T1 mapping and parameters of diastolic function.** Correlation between native T1 time and shear wave velocities (A),

pulmonary capillary wedge pressure (B) and E/E' (C), respectively. E/E'= mitral inflow to mitral relaxation velocity ratio, PCWP = pulmonary wedge pressure, SW = shear wave.

## TEXT TABLES

**Table 1: Baseline characteristics**

| *Clinical characteristics* | |
|---|---|
| *Variables* | *Values* |
| Age, years | 54.1 ± 17.8 |
| Male gender, n (%) | 36 (78) |
| Weight, kg | 73.9 ± 14.5 |
| Height, m | 1.75 ± 0.1 |
| BSA, $m^2$ | 1.9 ± 0.2 |
| Time since transplant, years | 9.9 ± 6.4 |
| Donor age, years | 35.5 ± 14.6 |
| Ischemic time during surgery, minutes | 2.8 [2.3, 3.5] |
| NYHA functional class, n (%) | |
| I | 35 (76) |
| II | 10 (22) |
| III or IV | 1 (2) |
| Hypertension, n (%) | 14 (30) |
| Diabetes mellitus, n (%) | 10 (22) |
| Stage of chronic kidney disease (CKDQI), n (%) | |
| Stage 1 | 2 (4) |
| Stage 2 | 12 (26) |
| Stage 3 | 11 (24) |
| Stage 4 | 7 (15) |
| Stage 5 | 2 (4) |
| *Electrocardiography* | |

| | |
|---|---|
| Rhythm, n (%) | |
| Sinus rhythm | 44(95.7) |
| Atrial pacing | 2(4.3) |
| AVB (first degree), n(%) | 1(2.2) |
| RBBB, n(%) | 9(26.1) |
| *Echocardiography* | |
| IVSd, mm | 13.3 ± 3.1 |
| SBP, mmHg | 138 ± 17 |
| DBP, mmHg | 84 ± 10 |
| Heart rate, beats/minutes | 79±11 |
| LVEDD, mm | 44.2 ± 6.2 |
| PW, mm | 9.9 ± 1.5 |
| LAV, ml | 95.3 ± 35.4 |
| LV EF, % | 59.6 ± 8.2 |
| LV Peak E wave, m/s | 0.85 ± 0.24 |
| LV Peak A wave, m/s | 0.39 ± 0.14 |
| LV E/A | 2.34 ± 0.83 |
| LV DT, ms | 177 ± 44 |
| LV E' average, m/s | 0.11 ± 0.03 |
| LV E/E' average | 8.3 ± 3.1 |
| LV IVRT, ms | 73.3 ± 31.8 |
| TV Vmax, m/s | 2.3 [2.0, 2.5] |
| GLS, % | -16.5 ± 2.6 |
| SW velocity at MVC m/s | 5.00 ± 2.04 |

| *Right heart catheterization* | |
|---|---|
| Heart rate, beats/minute | 77±12 |
| Cardiac index, l/min/$m^2$ | 2.9 [2.4, 3.1] |
| Right atrial pressure, mmHg | 8.4 ± 3.9 |
| Pulmonary artery mean pressure, mmHg | 21.9 ± 5.8 |
| Pulmonary artery systolic pressure, mmHg | 32.3 ± 8.7 |
| Pulmonary capillary wedge pressure, mmHg | 14.6 ± 5.2 |
| Pulmonary vascular resistance, dynes*sec/$cm^2$ | 120.5 ± 58.1 |
| *CMR* | |
| LV mass indexed, g/$m^2$ | 49.2 ± 12.2 |
| LV EF, % | 58.1 ± 5.8 |
| Non-contrast myocardial T1 time, ms | 1034 ± 41 |
| Non-contrast blood pool T1 time, ms | 1574 ± 106 |
| Post-contrast myocardial T1 time, ms | 410 ± 47 |
| Post-contrast blood pool T1 time, ms | 275 ± 53 |
| ECV, % | 0.28 ± 0.04 |
| T2 time, ms | 52 [50, 53] |

Values are mean ± SD, n/n (%), or median [IQR].

Abbreviations: A wave, late mitral valve inflow velocity; AVB, atrioventricular block; BMI, body mass index; BSA, body surface area; DBP, diastolic blood pressure; DT, deceleration time; E' average, average between septal and lateral mitral early relaxation velocity; E wave, early mitral valve inflow velocity; E/A, early to late mitral inflow velocity ratio; ECV, extracellular volume; E/E', mitral inflow to mitral relaxation velocity ratio; EF, ejection fraction; GLS, global longitudinal strain; IQR, interquartile range; IVRT, isovolumetric relaxation time; IVSd, interventricular septum at end-diastole; LAV, left atrial volume; LV,

left ventricle; LVEDD, left ventricular end-diastolic dimension; MVC, mitral valve closure; PW, posterior wall; RBBB, right bundle branch block; SD, standard deviation; SBP, systolic blood pressure; SW, shear wave; TV Vmax, maximal tricuspid regurgitation velocity;

**Table 2: Correlations between PCWP and echocardiographic parameters**

| *Parameter* | *r* | *p value* |
|---|---|---|
| SW velocity | 0.54 | **<0.001** |
| LAV | 0.43 | **0.005** |
| TVmax | 0.45 | **0.007** |
| Mean E/E' | 0.44 | **0.003** |
| DT | -0.26 | 0.09 |
| IVRT | 0.15 | 0.34 |
| E/A | 0.18 | 0.27 |

Abbreviations: DT, deceleration time; E/A, early to late mitral inflow velocity ratio; E/E', mitral inflow to mitral relaxation velocity ratio; IVRT, isovolumetric relaxation time; LAV, left atrial volume; SW, shear wave; TV Vmax, maximal tricuspid regurgitation velocity;

**Table 3: Correlations of diffuse myocardial injury**

| Parameter | *Native T1* | | *ECV* | |
|---|---|---|---|---|
| | r | p value | r | p value |
| ***Baseline characteristics*** | | | | |
| Ischemia donor heart | -0.45 | 0.06 | -0.27 | 0.27 |
| Time since transplant | -0.10 | 0.63 | 0.12 | 0.57 |
| ***Elastography*** | | | | |
| SW velocity | 0.75 | **0.0001** | 0.55 | **0.009** |
| ***Echocardiography*** | | | | |
| LAV | 0.44 | **0.04** | 0.39 | 0.09 |
| TVmax | 0.33 | 0.2 | 0.22 | 0.41 |
| E/E' | 0.35 | 0.1 | 0.36 | 0.1 |
| DT | -0.41 | 0.06 | -0.32 | 0.14 |
| IVRT | -0.17 | 0.43 | -0.10 | 0.65 |
| E/A | 0.27 | 0.22 | 0.38 | 0.08 |
| ***Cardiac catheterization*** | | | | |
| PCWP | 0.63 | **0.001** | 0.46 | **0.02** |
| RAP | 0.55 | **0.007** | 0.34 | 0.11 |
| sPAP | 0.72 | **<0.001** | 0.48 | **0.02** |

Abbreviations: A wave, late mitral valve inflow velocity; DT, deceleration time; E/A, early to late mitral inflow velocity ratio; ECV, extracellular volume; E/E', mitral inflow to mitral relaxation velocity ratio; IVRT, isovolumetric relaxation time; LAV, left atrial volume; LV, left ventricle; PCWP, pulmonary capillary wedge pressure; RAP, right atrial pressure; sPAP,

systolic pulmonary artery pressure; SW, shear wave; TV Vmax, maximal tricuspid regurgitation velocity;

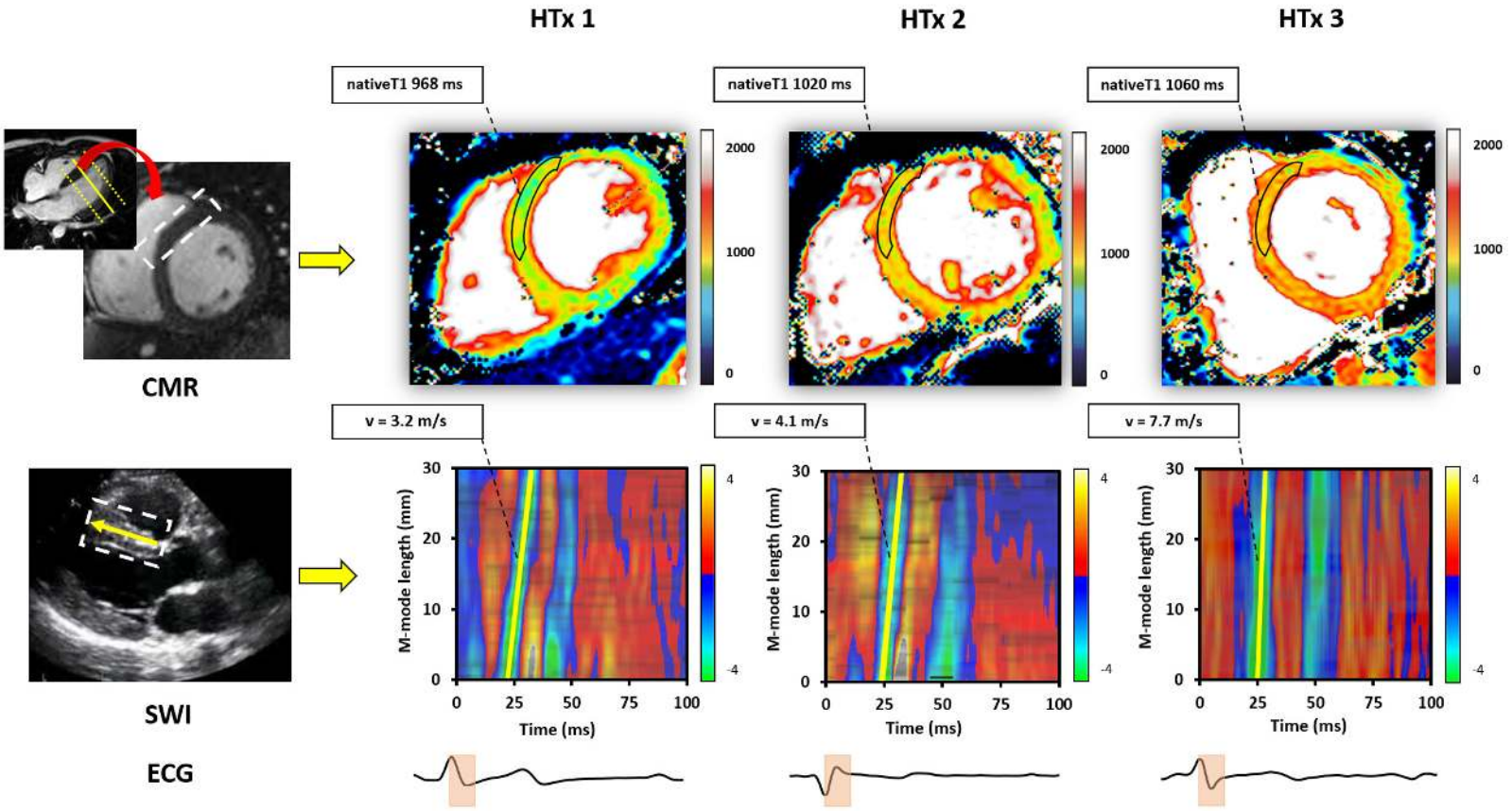
HTx 1
HTx 2
HTx 3
nativeT1 968 ms
nativeT1 1020 ms
nativeT1 1060 ms
2000
1000
0
CMR
v = 3.2 m/s
v = 4.1 m/s
v = 7.7 m/s
M-mode length (mm)
Time (ms)
4
-4
SWI
ECG

A.

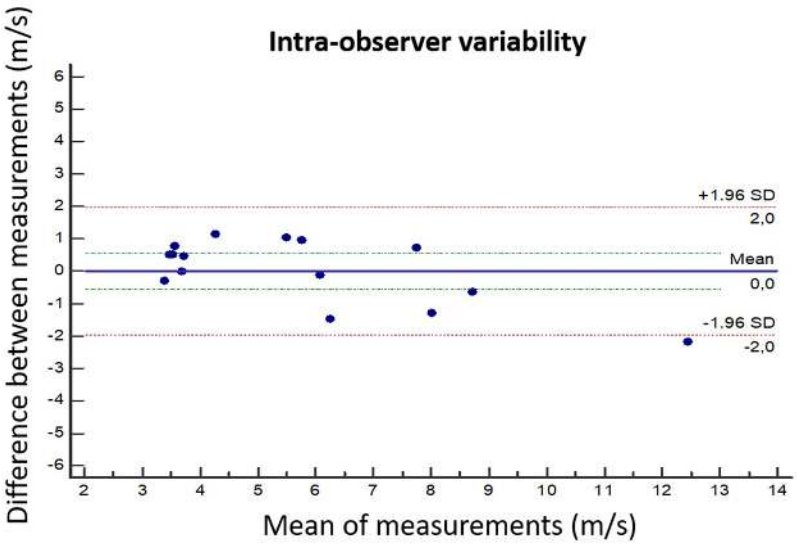
Intra-observer variability
Difference between measurements (m/s)
Mean of measurements (m/s)
+1.96 SD
2,0
Mean
0,0
-1.96 SD
-2,0

B.

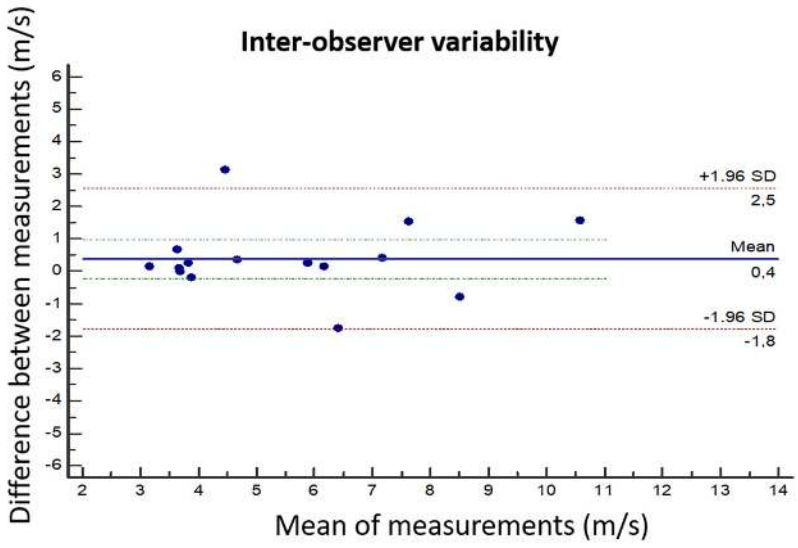
Inter-observer variability
Difference between measurements (m/s)
Mean of measurements (m/s)
+1.96 SD
2,5
Mean
0,4
-1.96 SD
-1,8

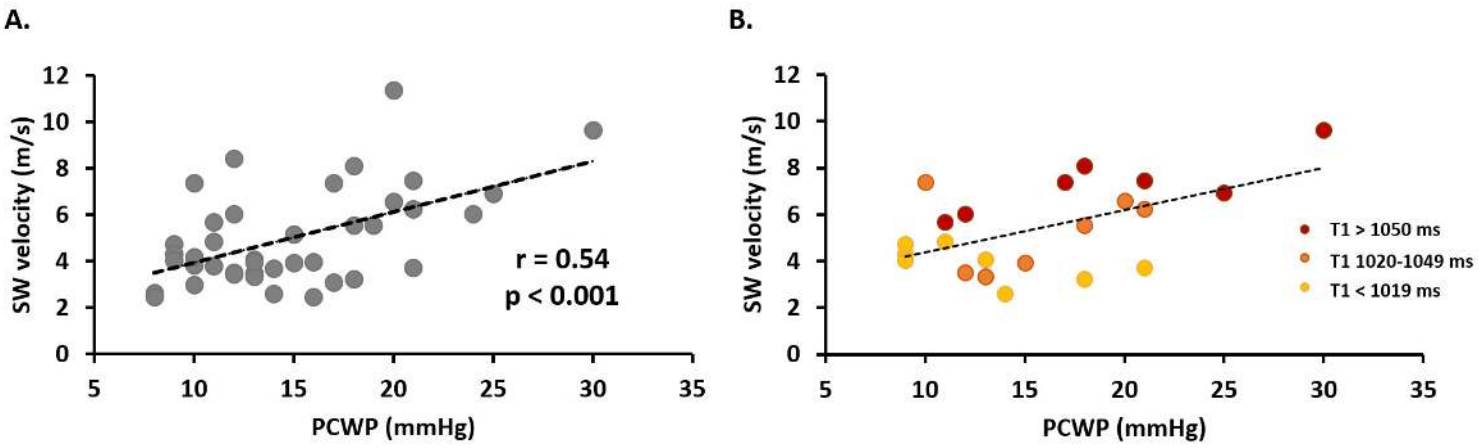
A.
B.
SW velocity (m/s)
PCWP (mmHg)
r = 0.54
p < 0.001
T1 > 1050 ms
T1 1020-1049 ms
T1 < 1019 ms

A.

Cut-off value: 5.14 m/s
Sensitivity = 71%
Specificity = 84%
AUC = 0.72
p = 0.01

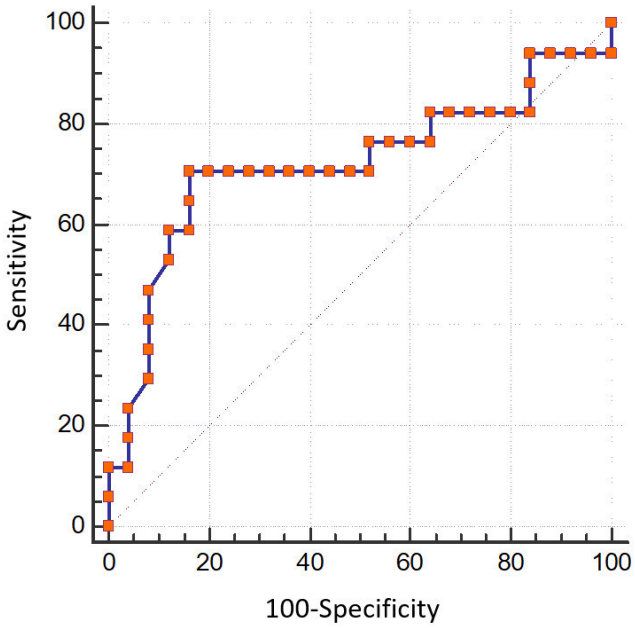


B.

Cut-off value: 4.84 m/s
Sensitivity = 82%
Specificity = 82%
AUC = 0.81
p = 0.001

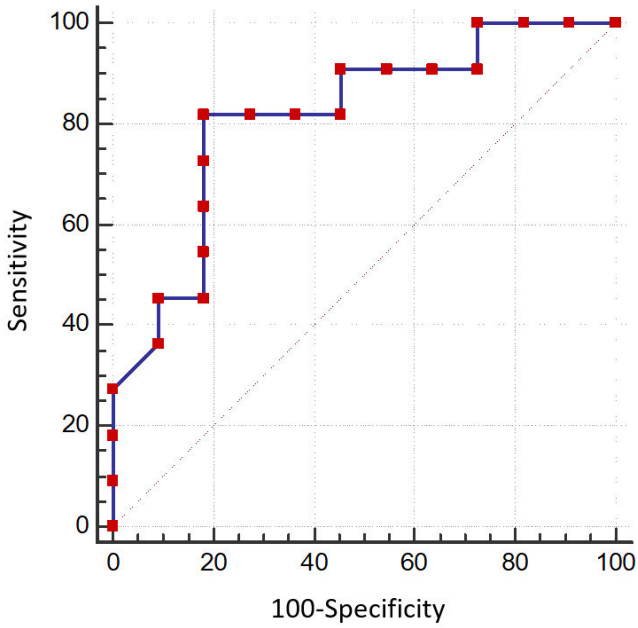

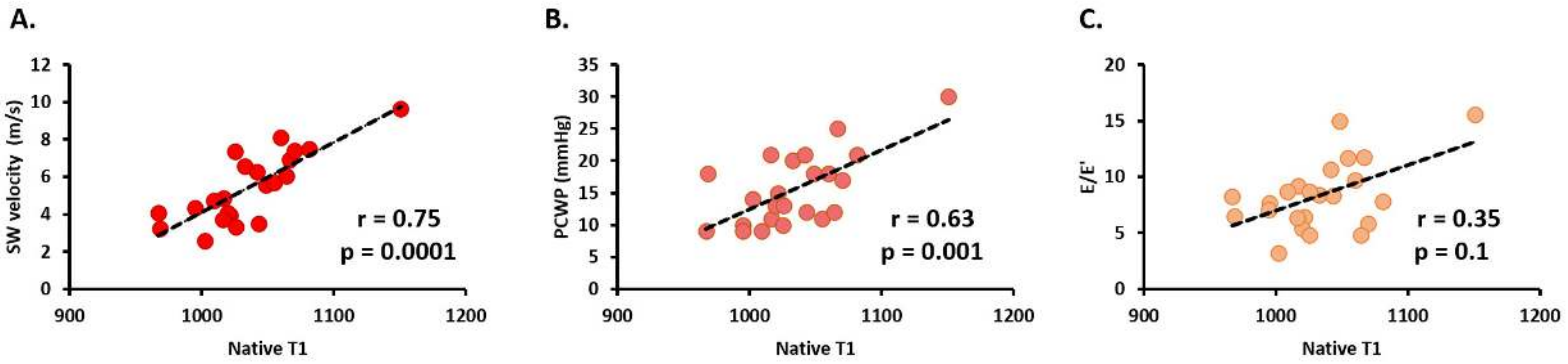
A.
SW velocity (m/s)
Native T1
r = 0.75
p = 0.0001
B.
PCWP (mmHg)
Native T1
r = 0.63
p = 0.001
C.
E/E'
Native T1
r = 0.35
p = 0.1